

1 **A Vital Sign-based Prediction Algorithm for Differentiating COVID-19 Versus Seasonal**
2 **Influenza in Hospitalized Patients**

3 Naveena Yanamala*^{1,2}, Nanda H. Krishna^{1,2}, Quincy A. Hathaway¹, Aditya Radhakrishnan^{1,2},
4 Srinidhi Sunkara^{1,2}, Heenaben Patel¹, Peter Farjo¹, Brijesh Patel¹, Partho P Sengupta*¹.

5 **Author Affiliations:** ¹Division of Cardiology, West Virginia University Medicine Heart &
6 Vascular Institute, Morgantown, WV; ²Institute for Software Research, School of Computer
7 Science, Carnegie Mellon University, Pittsburgh, PA

8 **Address of Correspondence:**

9

*Partho P. Sengupta, MD, DM	*Naveena Yanamala, MS, PhD
Heart & Vascular Institute	Heart & Vascular Institute
West Virginia University	West Virginia University
1 Medical Center Drive,	1 Medical Center Drive,
Morgantown, WV 26506	Morgantown, WV 26506
E-Mail: Partho.Sengupta@wvumedicine.org	E-Mail: naveena.yanamala.m@wvumedicine.org
Twitter: @ppsengupta1	Twitter: @YanamalaNaveena

10

11 **Abstract**

12 Patients with influenza and SARS-CoV2/Coronavirus disease 2019 (COVID-19) infections have
13 different clinical course and outcomes. We developed and validated a supervised machine
14 learning pipeline to distinguish the two viral infections using the available vital signs and
15 demographic dataset from the first hospital/emergency room encounters of 3,883 patients who
16 had confirmed diagnoses of influenza A/B, COVID-19 or negative laboratory test results. The
17 models were able to achieve an area under the receiver operating characteristic curve (ROC
18 AUC) of at least 97% using our multiclass classifier. The predictive models were externally
19 validated on 15,697 encounters in 3,125 patients available on TrinetX database that contains
20 patient-level data from different healthcare organizations. The influenza vs. COVID-19-positive
21 model had an AUC of 98%, and 92% on the internal and external test sets, respectively. Our
22 study illustrates the potentials of machine-learning models for accurately distinguishing the two
23 viral infections. The code is made available at [https://github.com/ynaveena/COVID-19-vs-](https://github.com/ynaveena/COVID-19-vs-Influenza)
24 [Influenza](https://github.com/ynaveena/COVID-19-vs-Influenza) and may be have utility as a frontline diagnostic tool to aid healthcare workers in
25 triaging patients once the two viral infections start cocirculating in the communities.

26

27 **Keywords:** Seasonal Influenza, Machine learning, Extreme gradient boosting trees.

28

29

30 **Word count (main text):** 3,437 (Limit 3,500); **Word count (methods):** 1,630 (Limit 3,000)

31

32

33 **Main**

34 Infection with severe acute respiratory syndrome coronavirus 2 (SARS-CoV 2) causing
35 coronavirus disease 2019 (COVID-19) has led to an unprecedented global crisis due to its
36 vigorous transmission, spectrum of respiratory manifestations, and vascular affects ¹⁻³. The
37 etiology of the disease is further complicated by a diverse set of clinical presentations, ranging
38 from asymptomatic to progressive viral pneumonia and mortality ⁴. Due to its similar
39 symptomatology, COVID-19 has drawn comparisons to the seasonal influenza epidemic.⁵ Both
40 infections commonly present with overlapping symptoms, leading to a clinical dilemma for
41 clinicians as SARS-CoV 2 carries a case-fatality rate up to 30 times that of influenza and infects
42 healthcare workers at a significantly higher rate.^{3,6,7} Moreover, the concurrence of epidemics
43 appears imminent as the considerable COVID-19 incidence continues and even a moderate
44 influenza season would result in over 35 million cases and 30,000 deaths.^{5,6} To help curb this
45 dilemma, front-line providers need the ability to rapidly and accurately triage these patients.

46 One approach to quickly classifying patients as COVID-19 positive or negative could be
47 through machine learning algorithms. While the use of machine learning has been applied to
48 contact tracing and forecasting during the COVID-19 epidemic ⁸, it has only limitedly been
49 explored as a means for accurately predicting COVID-19 infection on clinical presentation. With
50 just a few important parameters clinicians can diagnose the patients well before a laboratory
51 diagnosis. Preliminary work has shown the utility of machine and deep learning algorithms in
52 predicting COVID-19 for patient features ⁹⁻¹¹ and on CT examination ^{12,13}, but there remains a
53 paucity in research showing the capacity of machine learning algorithms in differentiating
54 between COVID-19 and influenza patients.

55 Vital signs are critical piece of information used in the initial triage of patients with
56 COVID-19 and/or influenza by care coordinators and health-care responders in community
57 urgent care centers or emergency rooms. It is becoming clearer that patient vital signs may
58 present uniquely in SARS-CoV 2 infection ⁹, likely as a result of alterations in gas exchange and
59 microvascular changes ¹⁴. In the present investigation, we therefore explored the use of machine
60 learning models to differentiate between SARS-CoV 2 and influenza infection using basic office-
61 based clinical variables. The use of simple ML-based classification may have utility for the rapid
62 identification, triage, and treatment of COVID-19 and influenza positive patients by front-line
63 healthcare workers, which is especially relevant as the influenza season approaches.

64

65 **Results**

66 **WVU Study Cohort**

67 *Baseline Characteristics*

68 The patient cohort included 3883 patients (mean age 52 ± 24 years, 48% males, and 89%
69 White/Caucasian) of whom 747 (19%) tested positive for SARSCoV-2 (COVID-19 positive
70 cohort), 1913 (49%) tested negative for SARSCoV-2 (COVID-19 negative cohort), and 1223
71 (31%) had influenza (Table 1). The majority of the COVID-19 positive and negative patients
72 were older; whereas the influenza cohort was younger ($P < 0.001$). There was higher prevalence
73 of Black/African Americans in the influenza cohort in comparison with other cohorts. COVID-
74 19 positive patients were more obese ($p < 0.001$). They also had higher mean temperature, systolic
75 and diastolic blood pressures than the other two cohorts ($p < 0.001$ for all variables). While the
76 Influenza cohort had higher mean body temperature, heart rate and oxygen saturations than

77 COVID-19-positive and -negative patients ($p < 0.001$). Patients in the COVID-19-positive and
78 influenza groups had a higher respiratory rate than the COVID-19-negative group (Table 1).

79 *Outcomes*

80 The overall mortality for the cohort was 6.7%. The crude case fatality rate was 6.8% in
81 the COVID-19-positive and 4.2% in influenza groups, with a 9.5% case fatality rate in the
82 COVID-19 negative group ($p < 0.001$). The COVID-19-positive patients had more than a 3-fold
83 higher rate for ICU admissions than patients with influenza (19.0% vs. 5.7%; $p < 0.001$), but the
84 rate was lower than the COVID-19 negative group (23.2%) ($p < 0.001$). The average age of
85 patients who died during hospitalizations was significantly higher in COVID-19 positive patients
86 (75 ± 14 years) compared to the influenza (69 ± 13 years) and COVID-19 negative groups ($72 \pm$
87 14 years) ($p = 0.02$), as presented in the Table 2.

88

89 **TriNetX Cohort**

90 The external cohort included a total of 15,697 patient encounters from 3,125 patients with
91 body temperature information available (Supplementary Table 2). This subgroup of the external
92 cohort included 6,613 encounters from 1,057 COVID-positive patients and 9,087 encounters
93 from 2,068 influenza patients. The COVID-19-positive group was predominantly male (54%),
94 while the influenza group involved more female (53%) patients. The COVID-19-positive group
95 included more Black/African-American (47%) patients, while the influenza cohort consisted of
96 more White/Caucasian (52%) patients. The vital signs for mean temperature, heart rate,
97 respiratory rate, and diastolic blood pressure showed a statistical difference between patients
98 with COVID-19 and those with influenza ($p < 0.0001$).

99 **COVID-19 Versus Influenza Infection Prediction at the ED or Hospitalization.**

100 In this study we explored the value of demographics, vitals and symptomatic features,
101 which are readily available to providers, in an effort to develop supervised machine learning
102 classifiers that can predict patients who are either COVID-19 positive or negative, while further
103 distinguishing influenza from COVID-19 infection. The WVU hospitalized patient cohort was
104 randomly divided into a training (80%) and testing set (20%) to develop four different contexts
105 specific XGBoost predictive models. We assessed receiver operator characteristic (ROC) area
106 under the curve (AUC) plots, precision, recall and other threshold evaluation metrics to select the
107 best performing model in each case (Tables 3, 4 & S3).

108 Panel A and B in Figure 1 shows the ROC curves for the prediction of influenza from
109 COVID-19 positive encounters and from those who are either COVID-19 positive or negative
110 obtained using the holdout test set. We present four unique models that can be used as a
111 framework to aid in the delineation between influenza and COVID-19 in the clinical setting. The
112 first model provided stratification of patients as either influenza or COVID-19 positive,
113 highlighted by a ROC AUC 98.8%, accuracy of 95%, sensitivity 94%, and specificity 95% at
114 identifying COVID-19-positive patients (Table 3). The second model distinguished influenza
115 patients from all other patients, irrespective of a patient's COVID-19 test, revealing an ROC
116 AUC of 98.7%, accuracy of 94%, sensitivity of 93%, and specificity of 94% (Figure 1, Panel B).
117 The third model distinguishes between COVID-19 positive and negative patients, with a ROC
118 AUC of 97.2%, accuracy of 92%, sensitivity of 85%, and specificity of 95% (Figure 2, Panel A
119 and Table 3). The Precision-Recall AUC was 94% for predicting COVID-19 positive versus
120 negative patients (Figure S2).

121 The fourth model employed a multi-class XGBoost framework trained to distinguish
122 between all three different types of patients had an ROC AUC of 98% and achieved 91%
123 precision at identifying patients that were positive for influenza with 91% recall, and 95%
124 precision at identifying those patients that tested negative for COVID-19 with a 88% recall.
125 While the highest specificity with precision was achieved when identifying COVID-19 positive
126 patients, the recall of 75% was significantly lower compared to other classes (91% for influenza
127 and 88% for COVID-19 negative patients). Average precision of the overall model was 91%,
128 accuracy was 90% and macro-average of ROC AUC was 97.6% (Figure 2 and Table S3).

129

130 **Importance of Various Features**

131 We use the Shapley Additive Explanations (SHAP) method ^{15,16}, specifically, using the
132 Tree Explainer method, to describe our XGBoost models.

133 *SHAP Importance*

134 SHAP is a model-agnostic interpretability method that aids in analyzing feature
135 importance based on their impact on the model's output. The additive importance of each feature
136 for the model is calculated over all possible orderings of features. Positive SHAP values indicate
137 a positive impact on the model's output, while negative values indicate negative impact on the
138 model's output. The most important features that identify patients with positive influenza
139 infection from others that are presented to ED included features such as age, body temperature,
140 body surface area (BSA) and heart rate (Figure 3A and B). Encounter-related features such as the
141 month of encounter along with reason for visit and encounter type also contributed to the most-
142 informative variables for predicting influenza compared to COVID-19 positive patients or

143 influenza vs all other patients (Figure 3). On the contrary, in the case of the COVID-19-positive
144 vs COVID-19 negative model, two vital signs i.e., body temperature and SPO₂ were amongst the
145 highest-ranking features. Age, BMI, diastolic blood pressure and encounter-related variables
146 such as reason for visit and month of encounter were additionally amongst the variables most
147 informative to model predictions. A similar trend of feature importance was also reflected in the
148 SHAP summary plot of the three-way multi-class classifier (Figure S1). Vital signs played a
149 more significant role in distinguishing between influenza and COVID-19 positive encounters
150 through parameters such as body temperature, heart rate and blood pressure.

151 From the SHAP summary plots (Figure 3 & S1), it is evident that the models captured
152 some important features and patterns that aid in correctly predicting Influenza and COVID-19-
153 positive encounters. These plots highlighted that patient encounters predicted to be COVID-19
154 positive are, on average, more likely to have lower heart rate, higher respiratory rate and lower
155 oxygen saturation. Lower blood oxygen saturation is known to be prevalent among COVID-19
156 patients and was identified by our machine learning models as an important feature for ,
157 validating the clinical appropriateness of our model design.

158 *Model Interpretability*

159 The SHAP force plots shown in Figures 4 & 5 aim to offer explanations for individual
160 predictions made by our models. The two plots generated for the COVID-19-positive vs
161 influenza classifier are shown in Figure 4. Panel A shows an encounter correctly classified as
162 influenza, with the month (during the time course of the traditional influenza season), BSA and
163 age (younger patient) values affecting the model output most. The effect of these features was
164 enough to prevent misclassification due to lower heart rate and SBP values. Panel B explains an
165 encounter correctly classified as COVID-19. While the encounter occurred in month 3, which

166 overlaps with the influenza season, the combined effect of higher age, low heart rate, BSA and
167 higher temperature pushes the prediction towards COVID-19, counteracting the effect of month
168 and encounter type.

169 Similarly, a second set of plots were generated for the COVID-19 positive vs negative
170 classifier (Figure 5). In these plots, Panel A shows an encounter correctly classified as COVID-
171 19 negative while Panel B shows an encounter classified correctly as COVID-19 positive. We
172 see in the former that the temperature, reason for visit, lower age and higher value of SPO₂ push
173 the prediction towards COVID-19 negative. In the latter, we see that the effect of temperature,
174 low SPO₂ value and higher age together counter the effect of the higher heart rate and normal
175 respiratory rate, to correctly classify the example as COVID-19 positive. With these
176 interpretability methods we are able to clearly determine the reasons for the model's output and
177 ensure they can be scrutinized. The insights obtained further corroborate with patterns often
178 observed in COVID-19 patients.

179

180 **Impact of Vitals on Model Performance**

181 *Stepwise removal of vitals based on feature importance.*

182 Each feature's importance to the construction of the machine learning model was assessed
183 through individually removing each vital sign parameter in the internal validation set. Stepwise
184 removal of vitals in the order of their importance of contribution to the multi-class classifier
185 (Figure S1) led to decrease in the performance of the model (Figure S3A). Removal of body
186 temperature significantly decreased models' performance to an accuracy of 74% and F1 score of

187 68% compared to the initial performance 90% and 89%, respectively. However, subsequent
188 removal of other vital signs, including heart rate did not affect model performance drastically.

189 *Inclusion of only one vital sign at a time.*

190 We also assessed how well the model performs given only one vital is present at a time in
191 the Internal test set. More specifically, when considering the importance of a given vital sign, all
192 other features related to vitals are removed from the internal test set. However, the demographics
193 and other information was not ablated. Figure S3B shows the models performance in terms of F1
194 score or statistic by only including one vital at a time. The higher the performance, the more
195 useful the vital sign is in helping the model to discriminate between COVID-19 and influenza
196 encounters. With the comparison of both multi-class classifier and COVID-19 positive vs
197 negative classifier performances, it is evident that body temperature has the greatest impact
198 among all vital signs considered. In addition to body temperature, heart rate was also seen to
199 contribute to the performance of COVID-19 positive vs negative model.

200 Taken together, these results suggest that of all the vital signs, body temperature,
201 followed by heart rate and SPO₂ could impact the predictive models' performance in
202 discriminating between influenza, COVID-19 positive and negative patient encounters.

203

204 **External Validation**

205 To further assess the generalizability of the predictive models and confirm the stability of
206 the model features at identifying patients positive for COVID-19 or influenza, we validated our
207 models using the TriNetX research network dataset external to WVU Medicine. Patients with
208 any missing data related to body temperature were excluded from the analysis. The dataset

209 included 6,613 encounters of COVID-19 patients (n=1,057) and 9,084 encounters related to
210 influenza patients (n=2,068). The influenza versus COVID-19 model demonstrated ROC AUC
211 of 92.3% with an accuracy of 85%, and 81% precision at identifying patients that were positive
212 for COVID-19 with 84% recall (Figure 1A & Table 4). Also, the model to detect patients with
213 influenza, irrespective of their COVID-19 status, showed similar performance with an AUC
214 ROC of 92.3% and an accuracy of 80% %, and 99% precision at identifying patients that were
215 positive for influenza with 68% recall (Figure 1B). This suggests that the developed models are
216 able to effectively identify patients across multiple TriNetX HCOs with influenza or COVID-19
217 infections amongst other COVID-19-negative patients presenting at ED and/or admitted to the
218 hospital.

219 Further, enforcing no missing values in the case of both heart rate and body temperature,
220 the two top ranked vital signs (Figure S3), did not result in boosting the performance. On the
221 contrary, restricting the data to have all vitals present, boosted the performance of ROC AUC to
222 and accuracy to 88% for the Influenza vs COVID-19 model and ROC AUC to and accuracy to in
223 the case of Influenza vs Other model (Table S4). These results suggest that while enforcing no
224 missing values in vitals could support a better overall model performance (i.e., AUC ROC 94.3%
225 vs 92.3%), missingness in most of the vitals does not seem to limit its applicability and
226 generalizability.

227

228 **Discussion**

229 This investigation provides a machine-learning pipeline with a multi-step framework to
230 differentiate between COVID-19 and influenza. Further, this is the first machine learning model

231 to leverage a patient population that includes both the initial (February-April) and secondary
232 (May-September) surge of SARS-CoV 2 infections in the United States ¹⁷. Our approach can
233 guide future applications, highlighting the importance of developing dynamic models that control
234 for confounding comorbidities, such as influenza, and the ever-evolving infectivity of SARS-
235 CoV 2. Importantly, as influenza season approaches it will be of high priority to establish a
236 reliable process for identifying patients at risk of COVID-19, influenza, or other viral infections
237 to increase the prognostic value of a directed therapy.

238 While the initial presentation of COVID-19 and influenza appear similar, the number,
239 and combination, of signs and symptoms can help provide better stratification. From a symptom
240 standpoint, COVID-19 causes more fatigue, diarrhea, anosmia, acute kidney injury, and
241 pulmonary embolisms, while sputum production and nasal congestion are more specific to
242 influenza ¹⁸. Furthermore, COVID-19 tends to cause worse decompensation. For instance, out of
243 200 cases of either influenza or COVID-19 in a study from France, only COVID-19 resulted in
244 severe respiratory failure requiring intubation¹⁸. Our evaluation revealed that the month the
245 patient was seen, age, and heart rate were the most important features for predicting a diagnosis
246 of COVID-19 over that of influenza infection. Additionally, body temperature and SPO₂ were
247 two of the most important features that indicated if a patient would be positive or negative for
248 COVID-19, which is likely a result of the underlying pathophysiology of the virus. SARS-CoV 2
249 infection appears to cause more significant endothelial dysfunction and systemic inflammation
250 likely leading to the worse case-fatality rate.^{6,19} These differences can be seen histologically as
251 well. Autopsy samples of COVID-19 lung tissue showed severe endothelial injury and
252 widespread thrombosis with microangiopathy ²⁰. These samples had nine times as much alveolar

253 capillary microthrombi compared to that of influenza lung tissue and even showed evidence of
254 new vessel growth through a mechanism of intussusceptive angiogenesis ^{1,20}.

255 Machine learning algorithms can provide distinct advantages in the classification of
256 positive COVID-19 cases as the virus, and the demographic it infects, continues to evolve. The
257 West Virginia University (WVU) cohort consists of a fairly homogenous population, with 89%
258 of the population identifying as White/Caucasian and only 5% as Black/African American.
259 While our machine learning models were built around the WVU cohort, they demonstrate robust
260 performance even on more racially/ethnically diverse populations, such as in the TriNetX
261 dataset, when predicting patients who have influenza or COVID-19 (ROC AUC = 94.3%) and
262 influenza only (ROC AUC = 96.2%). The generalizability of our model may suggest that
263 features that define SARS-CoV 2 infection (e.g., age, heart rate, body temperature, SPO₂) could
264 represent similarities in clinical presentation, regardless of a patient's race/ethnicity. Further
265 understanding the socioeconomic ^{21,22} and physiological ^{23,24} differences in minority populations
266 will be important in determining why COVID-19 disproportionately affects these populations
267 and how machine learning models can more accurately model heterogeneous populations.

268 Patient information provided in the WVU and TriNetX datasets consists of both the
269 initial rise in cases in the United States (February-April) as well as a secondary surge (May-
270 September). The second surge of infections shifted demographically from a predominately older
271 population to one with the highest prevalence between ages 20-29, with an increased rate of mild
272 to asymptomatic presentations ²⁵. Additionally, SARS-CoV 2 is an RNA virus with the capacity
273 to mutate. Sequencing studies have already identified a variety of genetic variants, with most
274 mutations currently having no clear association with a positive or negative selective virulence ²⁶.
275 Though, some mutations, such as D614G, are suggested to increase infectivity of SARS-CoV 2

276 and outcompete other strains in the environment ²⁷. Regardless, in our current approach, applying
277 machine learning over the continuum of the COVID-19 epidemic provides distinct advantages in
278 producing a generalizable model for continued use, which may not be captured in models
279 generated on earlier datasets.

280 The current study provides robust ROC AUC prediction of patients with COVID-19
281 (98.3%), without COVID-19 (97.4%), and those with influenza (97.1%) in our multi-class
282 model. While only demographic information and vital signs were applied to our models, overall
283 prediction could likely improve with the addition of other features including biochemical,
284 metabolic, and molecular markers, as well as imaging modalities such as X-ray and CT. The
285 addition of these features could likely improve diagnostic accuracy and should be tested in future
286 studies delineating between COVID-19 and influenza. Additionally, the current investigation
287 involves influenza and COVID-19 data from non-overlapping periods (i.e., influenza from winter
288 2019 and COVID-19 from spring/summer/fall 2020). Although some of the machine learning
289 models rely on time of presentation for prediction, we anticipate that the four-model framework
290 provided in the study will sufficiently stratify patients even when influenza season and the
291 COVID-19 epidemic overlap. This is reinforced by the prediction of COVID-19 positive and
292 negative cases (ROC AUC = 97.2%) in our model, which did not rely on time of presentation as
293 a variable.

294

295 Our study was limited by the classification of patients in the internal (WVU) and external
296 (TriNetX) datasets. While the WVU cohort includes patients, who have been confirmed to have a
297 negative SARS-CoV 2 test on presentation, the TriNetX dataset does not have this information.
298 Both datasets are also unable to capture patients with other respiratory viruses and viral

299 coinfections; information that could better explain variations in COVID-19 clinical presentation.
300 Another limitation is the need to continually adjust these models to fit new trends in SARS-CoV
301 2 spread and infectivity. Our models benefit from the inclusion of data spanning from February
302 to October, which can better simulate the current COVID-19 epidemic and influenza season but
303 will still require future iterations and validations to accurately predict SARS-CoV 2 infections.
304 Further, an understanding of COVID-19 and viral co-infections is needed to appropriately model
305 the risks of patients presenting with both illnesses²⁸⁻³⁰.

306

307 **Conclusions**

308 Here we highlight how machine learning can effectively classify influenza and COVID-
309 19 positive cases through vital signs on clinical presentation. This work is the first step in
310 building a low-cost, robust classification system for the appropriate triage of patients displaying
311 symptoms of a viral respiratory infection. With these algorithms, the identification of proper
312 treatment modalities for both COVID-19 and influenza can be made more rapidly, increasing the
313 effectiveness of patient care.

314

315 **Outlook**

316 We certainly hope that our current work can aid healthcare workers and clinicians to rapidly
317 identify, triage, and guide treatment decisions when the two viral infections start cocirculating in
318 the communities. In addition, Further studies validating the model as we see more coinfection in
319 an upcoming season can significantly improve the quality of care and proper allocation of
320 resources during this global pandemic.

321

322

323 **Materials and Methods**

324 **WVU Internal Cohort Dataset**

325 De-identified clinical and demographics data for all patients presenting to the emergency
326 department and/or admitted at West Virginia University hospitals between January 1st, 2019, and
327 November 4th, 2020, were extracted and provided to us by WVU Clinical and Translational
328 Science Institute (CTSI). The COVID-19 positive dataset includes all patients who had a lab-
329 based diagnostic test positive for SARS-CoV-2 at WVU Medicine between March 1st, 2020, and
330 November 4th, 2020 and had an associated hospital encounter with all vital signs information
331 available. The influenza positive dataset includes a random sample of 1500 patients who had a
332 lab-based diagnostic test that was positive for either Influenza Type A or Influenza Type B at
333 WVU Medicine between January 1st, 2019, and November 3rd, 2020, and had a hospital
334 encounter associated with that positive test. The COVID-19 negative dataset includes a random
335 sample of 2000 patients who had negative test results for SARS-CoV-2 and who never had a
336 positive diagnostic test for SARS-CoV-2 at WVU Medicine between March 1st, 2020, &
337 November 4th, 2020 provided that an associated hospital encounter occurred with that negative
338 test. As our study aims to create a model that can accurately discriminate COVID-19 from
339 influenza patients solely based on the patient's demographic information and vital signs data,
340 patients with any of the vital signs missing during the associated encounters were therefore
341 excluded from the analysis. This resulted in a final WVU cohort that included a total of 747
342 COVID-19 positive, 1223 influenza and 1913 COVID-19 negative patients (Table 1).

343

344

345 **TriNetX External Cohort Dataset**

346 The external validation cohort was obtained from the TriNetX Research network, a
347 cloud-based database resource that provides researchers access to de-identified patient data from
348 networks of healthcare organizations (HCO), mainly from large academic centers and other data
349 providers. The data is directly pulled from electronic medical records and accessible in a de-
350 identified manner. The TriNetX database includes patient-level demographic, vital signs,
351 diagnoses, procedures, medications, laboratory, and genomic data. For this study, we identified
352 COVID-19 and influenza cases using the International Classification of Diseases, 10th revision.
353 We used ICD-10 codes J9.0, J10.0, J09.*, and J10.* for influenza, and U07.1 for COVID-19.
354 Cases from February 1st, 2020, to August 13th, 2020, were queried and extracted. Due to
355 heterogeneity in reporting of COVID-19 testing (i.e., positive vs. negative; normal vs. abnormal),
356 we refrained from selecting the patients based on their testing results and used diagnostic codes
357 instead. Thus, we were only able to extract COVID-19 positive and influenza positive patients
358 for external validation. Further patients at least 18 years or older at the time of diagnosis and
359 their encounters defined as an encounter occurring within 7days from the date of diagnosis were
360 enforced to be included in the final cohort (n=34,670). Enforcing no missing values
361 corresponding to body temperature resulted in a dataset (n=15,697) that had a total of 6,613
362 (n=1057 patients) and 9084 (n=2068 patients) encounters diagnosed with COVID-19 and
363 Influenza, respectively. Baseline characteristics of the cohort is described in Supplementary
364 Table 2. Since the TriNetX data is de-identified, Institutional Board Review (IRB) oversight is
365 not necessary.

366

367

368 **Data Preprocessing & Split**

369 Different clinical variables investigated in this study include (a) vital signs i.e., body
370 temperature, heart rate, breathing/respiratory rate, oxygen saturation or SPO₂ and blood pressure,
371 (b) encounter date/type, (c) reason for visit, and (d) basic demographics information such as Age,
372 Gender, Race, and Ethnicity. Of the features considered, the data elements corresponding to sex
373 and ethnicity were binarized for being “female” and “Hispanic or Latino”, respectively. The race
374 feature was further one-hot encoded to three variables i.e., race_White/Caucasian,
375 race_Black/African American and race_Other. Finally, the date of the encounter was converted
376 to represent a numerical value for month, rather than specific day/year to remove the granularity
377 and capture the seasonal effects of influenza.

378

379 **Predictive Model Development using Extreme Gradient Boosting Trees**

380 *Model Training and Testing*

381 XGBoost, a gradient-boosted tree algorithm, was used to develop classifiers to
382 distinguish between patient encounters with confirmed COVID-19 from that of either influenza
383 patient encounters or other unknown viral infections. Separate models were developed to predict
384 confirmed COVID-19 patient encounters post Feb 1, 2020 from either influenza and/or those that
385 tested negative for COVID-19 (i.e., COVID-19 positive vs influenza, COVID-19 positive vs
386 COVID-19 negative, COVID-19 positive vs influenza vs COVID-19 negative), and then an
387 additional model to test influenza infections from others i.e., patients that were either positive or
388 negative to a COVID-19 test (Influenza vs Others). For the purpose of model training and
389 testing, we only consider data from 01-Feb-2020 until 04-Nov-2020 for COVID-19 positive and

390 negative cohorts and from 01-Jan-2019 to 04-Nov-2020 for the influenza patient cohort. We
391 partitioned the dataset into training and testing sets, using an 80%–20% split. The holdout test, or
392 internal validation, set is never seen by the model during training and was used only during
393 performance evaluation.

394 Gradient-boosted trees were selected due to their ability to model complex nonlinear
395 relationships, while robustly handling outliers and missing values. Gradient-boosted trees fuse
396 the concepts of gradient descent (in the loss function space) and boosting. Simpler tree-based
397 models are built additively like a boosting ensemble, to fit the gradient of the loss function for
398 every data point. Only a fraction of the trees fit to the gradient of the loss per data point in the
399 training set. This is analogous to small steps of gradient descent in the loss function space.

400 For developing the COVID-19 positive vs negative, Influenza vs Others and COVID-19
401 vs Influenza XGBoost models, the value of learning rate was set to 0.02 and the total number of
402 trees was 600. The alpha value was set to 0 and lambda was set to 1, i.e., we use L2
403 regularization. Further, min_child_weight was set to 1, to allow highly specific patterns to be
404 learnt as well. To counter the possibility of overfitting, the max_depth parameter of the XGBoost
405 model was set to 4, as more complex features are learnt with higher depths, leading to poor
406 performance on the unseen data. We used the gain importance metric to decide node splits for
407 the tree estimator, and the objective was set to binary logistic regression. The model outputs the
408 predicted probability, and records whose probability was at least 0.5 were considered as
409 belonging to the positive class, while others were deemed to belong to the negative class.
410 Further, the subsample parameter of the XGBoost algorithm represents the ratio of the records to
411 be sampled before forming a tree and was set to a value of 0.8. Similarly, the colsample_bytree
412 parameter which determines the fraction of columns to be sampled before every tree formation

413 was set to 1, meaning all features are used. Only records with all vitals were considered, however
414 the model does have the ability to make predictions in the absence of certain features. The
415 `compute_sample_weight` from the `sklearn.utils.class_weight` library was employed to ensure that
416 each training sample is weighted based on its class, to counter imbalance in the dataset.

417 For the three-class classifier that discriminates between COVID-19-positive, COVID-19-
418 negative and Influenza encounters, we developed an XGBoost model of 100 trees, with
419 `learning_rate` set to 0.3 and `max_depth` fixed at 6. The objective was set to `softprob` (uses a
420 softmax objective function), to perform multi-class classification. Furthermore, the `subsample`
421 parameter was set to 1, meaning all samples were used to form trees. No sample weighting was
422 carried out for this model. All other parameters remained the same as the models discussed
423 previously.

424 *Model Validation*

425 We also consider an unseen external validation dataset (TriNetX cohort) to evaluate the
426 performance of the model on data that is completely different from what it is accustomed to
427 during training. Patient-wise encounters with no missing vitals were enforced to test and evaluate
428 the performance of the developed models.

429 *Performance Evaluation Metrics*

430 The discriminative ability of each of the models developed in predicting patients with
431 influenza from COVID-19 positive and /or negative patients as well as those with a positive
432 COVID-19 test from negative test was evaluated in the hold-out test set and an external
433 validation test by using receiver operator characteristic (ROC) curve analysis. An area under the
434 curve (AUC) ≥ 0.5 indicated better predictive values. The closer the AUC was to 1, the better

435 the model's performance was. Additionally, "classification accuracy", the total number of true
436 positive scores i.e. when predicted values are equal to the actual values given by the attribute
437 positive predictive value (PPV) or "precision" score, "recall" which is the total number of true
438 positive instances among all the positive instances, and "F1 score" the weighted harmonic mean
439 of precision and recall along with negative predictive value (NPV) were estimated to evaluate
440 performance and the overall generalizability of each of the models. Further details on the
441 calculations of different metrics employed are provided in Supplementary methods.

442

443 **Statistical analysis**

444 We performed the Shapiro-Wilk test on the entire WVU internal cohort dataset to check
445 for normalcy of the data. We found that all the variables were normally distributed; therefore, we
446 used parametric methods for further statistical analysis. Categorical data are presented as counts
447 (percentages) while continuous data were reported as mean \pm standard deviation (SD). To
448 determine the significance of continuous variables between all three different groups (i.e.,
449 COVID-19 positive, influenza, and COVID-19 negative) Kruskal-Wallis test with Dunn-
450 Bonferroni correction test was used. The comparison between two of these three groups
451 (COVID-19 positive vs negative, COVID-19 positive vs influenza, influenza vs COVID-19
452 negative) to determine significance was performed using an independent sample t-test. Chi-
453 square was used for the categorical variable because the expected value for each cell is greater
454 than 5. All statistical analysis was performed using Medcalc for Windows, version 19.5.3
455 (MedCalc Software, Ostend, Belgium), and python for windows, version 3.8.3. A statistical
456 significance level of $p < 0.05$ was used for all the tests performed.

457

458 **Data Availability Statement**

459 The data that support the findings of this study are available from WVU CTSI & TriNetX but
460 restrictions apply to the availability of these data, which were used under license for the current
461 study, and so are not publicly available. Data is however available from the authors upon
462 reasonable request and with permission of WVU CTSI & TriNetX.

463

464 **Code availability**

465 The code is made available at <https://github.com/ynaveena/COVID-19-vs-Influenza> for non-
466 commercial use.

467

468 **References**

- 469 1 Ackermann, M. *et al.* Pulmonary Vascular Endothelialitis, Thrombosis, and Angiogenesis in
470 Covid-19. *N Engl J Med* **383**, 120-128, doi:10.1056/NEJMoa2015432 (2020).
- 471 2 Li, Q. *et al.* Early Transmission Dynamics in Wuhan, China, of Novel Coronavirus-Infected
472 Pneumonia. *N Engl J Med* **382**, 1199-1207, doi:10.1056/NEJMoa2001316 (2020).
- 473 3 Zhu, N. *et al.* A Novel Coronavirus from Patients with Pneumonia in China, 2019. *N Engl J Med*
474 **382**, 727-733, doi:10.1056/NEJMoa2001017 (2020).
- 475 4 Lee, Y. H., Hong, C. M., Kim, D. H., Lee, T. H. & Lee, J. Clinical Course of Asymptomatic and Mildly
476 Symptomatic Patients with Coronavirus Disease Admitted to Community Treatment Centers,
477 South Korea. *Emerg Infect Dis* **26**, 2346-2352, doi:10.3201/eid2610.201620 (2020).
- 478 5 Gostin, L. O. & Salmon, D. A. The Dual Epidemics of COVID-19 and Influenza: Vaccine
479 Acceptance, Coverage, and Mandates. *JAMA* **324**, 335-336, doi:10.1001/jama.2020.10802
480 (2020).
- 481 6 Solomon, D. A., Sherman, A. C. & Kanjilal, S. Influenza in the COVID-19 Era. *JAMA*,
482 doi:10.1001/jama.2020.14661 (2020).
- 483 7 Zayet, S. *et al.* Clinical features of COVID-19 and influenza: a comparative study on Nord
484 Franche-Comte cluster. *Microbes Infect*, doi:10.1016/j.micinf.2020.05.016 (2020).

- 485 8 Lalmuanawma, S., Hussain, J. & Chhakchhuak, L. Applications of machine learning and artificial
486 intelligence for Covid-19 (SARS-CoV-2) pandemic: A review. *Chaos Solitons Fractals* **139**, 110059,
487 doi:10.1016/j.chaos.2020.110059 (2020).
- 488 9 Soltan, A. A. S. *et al.* Artificial intelligence driven assessment of routinely collected healthcare
489 data is an effective screening test for COVID-19 in patients presenting to hospital.
490 doi:<https://doi.org/10.1101/2020.07.07.20148361>; (2020).
- 491 10 Sun, L. *et al.* Combination of four clinical indicators predicts the severe/critical symptom of
492 patients infected COVID-19. *J Clin Virol* **128**, 104431, doi:10.1016/j.jcv.2020.104431 (2020).
- 493 11 Wu, J. *et al.* Rapid and accurate identification of COVID-19 infection through machine learning
494 based on clinical available blood test results. *medRxiv*,
495 doi:<https://doi.org/10.1101/2020.04.02.20051136>; (2020).
- 496 12 Ardakani, A. A., Kanafi, A. R., Acharya, U. R., Khadem, N. & Mohammadi, A. Application of deep
497 learning technique to manage COVID-19 in routine clinical practice using CT images: Results of
498 10 convolutional neural networks. *Comput Biol Med* **121**, 103795,
499 doi:10.1016/j.compbio.2020.103795 (2020).
- 500 13 Ozturk, T. *et al.* Automated detection of COVID-19 cases using deep neural networks with X-ray
501 images. *Comput Biol Med* **121**, 103792, doi:10.1016/j.compbio.2020.103792 (2020).
- 502 14 Diehl, J. L. *et al.* Respiratory mechanics and gas exchanges in the early course of COVID-19 ARDS:
503 a hypothesis-generating study. *Ann Intensive Care* **10**, 95, doi:10.1186/s13613-020-00716-1
504 (2020).
- 505 15 Lundberg, S. M., Lee Su-In in *31st Conference on Neural Information Processing Systems (NIPS*
506 *2017), Long Beach, CA, USA*.
- 507 16 Lundberg, S. M. *et al.* From Local Explanations to Global Understanding with Explainable AI for
508 Trees. *Nat Mach Intell* **2**, 56-67, doi:10.1038/s42256-019-0138-9 (2020).
- 509 17 Roser, M., Ritchie, H., Ortiz-Ospina, E. & Hasell, J. (Published online at OurWorldInData.org,
510 2020).
- 511 18 Faury, H. *et al.* Medical features of COVID-19 and influenza infection: A comparative study in
512 Paris, France. *J Infect*, doi:10.1016/j.jinf.2020.08.017 (2020).
- 513 19 Vardeny, O., Madjid, M. & Solomon, S. D. Applying the Lessons of Influenza to COVID-19 During
514 a Time of Uncertainty. *Circulation* **141**, 1667-1669, doi:10.1161/CIRCULATIONAHA.120.046837
515 (2020).
- 516 20 Calabrese, F. *et al.* Pulmonary pathology and COVID-19: lessons from autopsy. The experience of
517 European Pulmonary Pathologists. *Virchows Arch* **477**, 359-372, doi:10.1007/s00428-020-02886-
518 6 (2020).
- 519 21 Chowkwanyun, M. & Reed, A. L., Jr. Racial Health Disparities and Covid-19 - Caution and
520 Context. *N Engl J Med* **383**, 201-203, doi:10.1056/NEJMp2012910 (2020).
- 521 22 Selden, T. M. & Berdahl, T. A. COVID-19 And Racial/Ethnic Disparities In Health Risk,
522 Employment, And Household Composition. *Health Aff (Millwood)* **39**, 1624-1632,
523 doi:10.1377/hlthaff.2020.00897 (2020).
- 524 23 Fei, K. *et al.* Racial and Ethnic Subgroup Disparities in Hypertension Prevalence, New York City
525 Health and Nutrition Examination Survey, 2013-2014. *Prev Chronic Dis* **14**, E33,
526 doi:10.5888/pcd14.160478 (2017).
- 527 24 Forde, A. T. *et al.* Discrimination and Hypertension Risk Among African Americans in the Jackson
528 Heart Study. *Hypertension* **76**, 715-723, doi:10.1161/HYPERTENSIONAHA.119.14492 (2020).
- 529 25 Boehmer, T. K. *et al.* Changing Age Distribution of the COVID-19 Pandemic - United States, May-
530 August 2020. *MMWR Morb Mortal Wkly Rep* **69**, 1404-1409, doi:10.15585/mmwr.mm6939e1
531 (2020).

- 532 26 Day, T., Gandon, S., Lion, S. & Otto, S. P. On the evolutionary epidemiology of SARS-CoV-2. *Curr*
533 *Biol* **30**, R849-R857, doi:10.1016/j.cub.2020.06.031 (2020).
- 534 27 Zhang, L. *et al.* The D614G mutation in the SARS-CoV-2 spike protein reduces S1 shedding and
535 increases infectivity. *bioRxiv*, doi:10.1101/2020.06.12.148726 (2020).
- 536 28 Ding, Q., Lu, P., Fan, Y., Xia, Y. & Liu, M. The clinical characteristics of pneumonia patients
537 coinfecting with 2019 novel coronavirus and influenza virus in Wuhan, China. *J Med Virol*,
538 doi:10.1002/jmv.25781 (2020).
- 539 29 Miatech, J. L., Tarte, N. N., Katragadda, S., Polman, J. & Robichaux, S. B. A case series of
540 coinfection with SARS-CoV-2 and influenza virus in Louisiana. *Respir Med Case Rep* **31**, 101214,
541 doi:10.1016/j.rmcr.2020.101214 (2020).
- 542 30 Zhou, X. *et al.* The Outbreak of Coronavirus Disease 2019 Interfered with Influenza in Wuhan
543 *SSRN*, doi:<http://dx.doi.org/10.2139/ssrn.3555239> (2020).

544

545

546 **Acknowledgements**

547 The authors acknowledge Matthew Armistead, Emily Morgan, Maryam Khodaverdi, and Wes
548 Kimble for their support with data collection and providing de-identified datasets.

549

550 **Funding Information:** This work is supported in part by funds from the National Science
551 Foundation (NSF: # 1920920) National Institute of General Medical Sciences of the National
552 Institutes of Health under (NIH: #5U54GM104942-04). The content is solely the responsibility
553 of the authors and does not necessarily represent the official views of the National Institutes of
554 Health or National Science Foundation.

555

556 **Author Contributions**

557 P.P.S and NY envisioned and designed the projects. NY, N.H.K, AR, and SS performed machine
558 learning modeling and analysis. P.P.S., Q.A.H, BP, and PF was involved with clinical
559 interpretation of the findings and writing as well as editing the manuscript. H.B.P and S.S.

560 performed the statistical analysis. All the authors have significantly been involved in the drafting
561 of the manuscript or revising it critically for important intellectual content.

562 **Competing Interests**

563 The authors declare the following competing interests. Dr. Sengupta is a consultant for
564 HeartSciences, Kencor Health and Ultromics. The remaining authors declare no competing
565 interests.

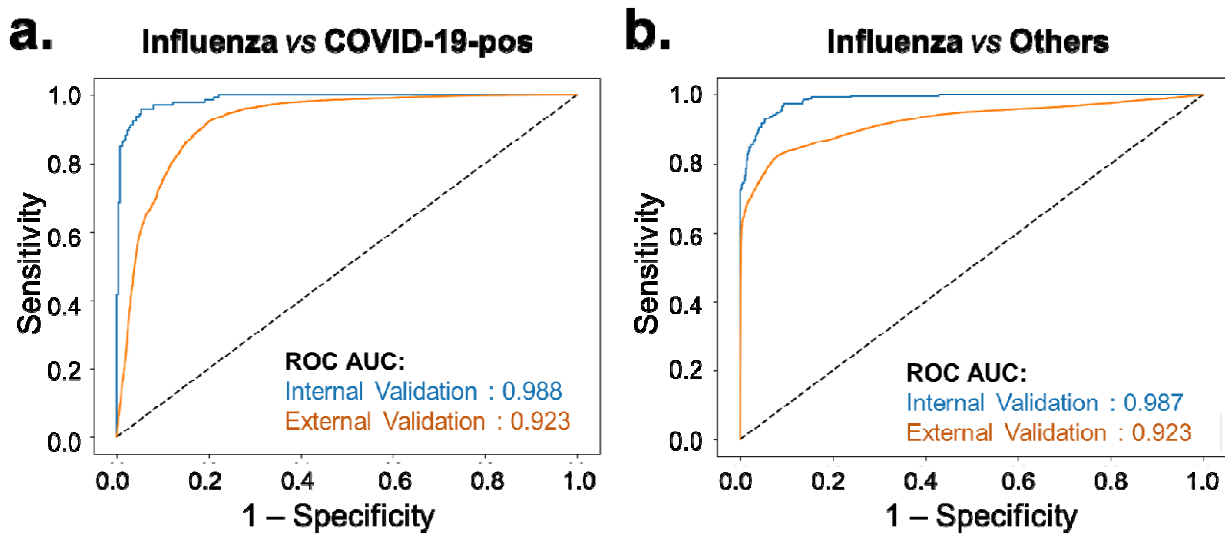
566

567 **Figures.**

568

569 **Figure 1.** Receiver Operating Characteristic Curves showing the predictive performance of the
570 (a) influenza versus COVID-19-positive model and (b) Influenza versus Other prediction models

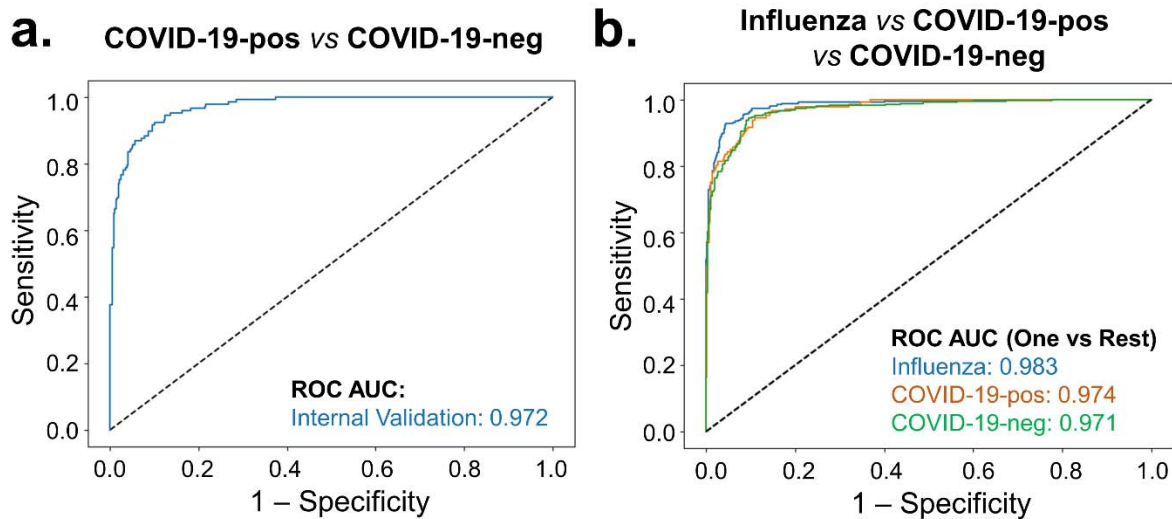
571 on the internal test and external validation datasets.



572

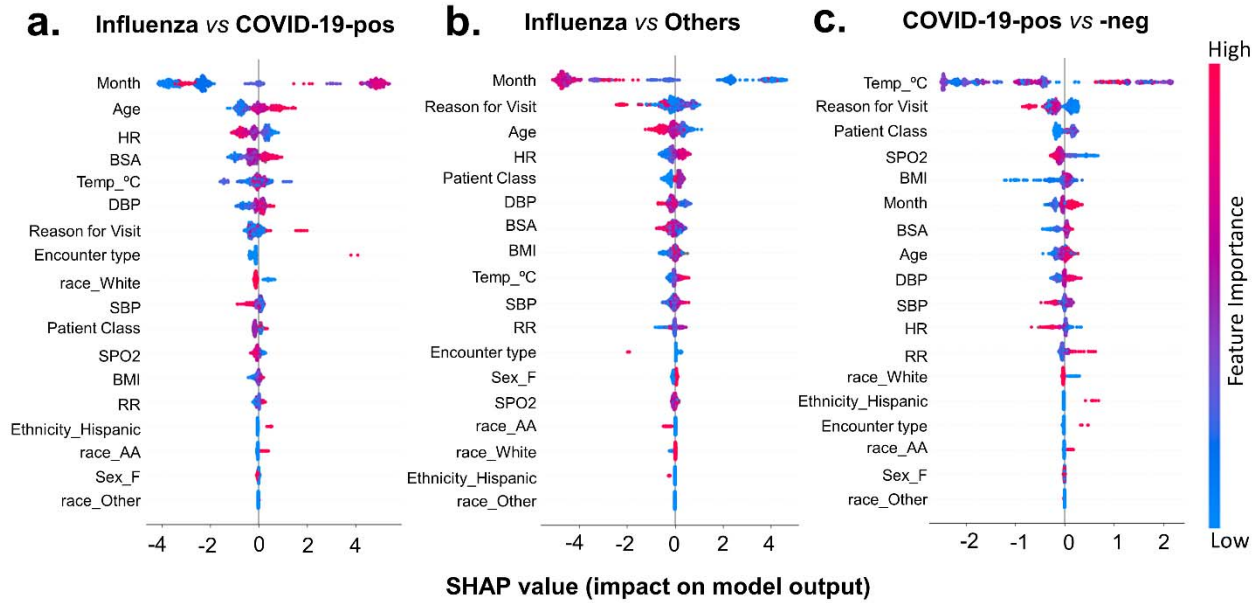
573

574 **Figure 2.** Receiver Operating Characteristic Curves showing the predictive performance of the
575 (a) COVID-19-positive versus COVID-19-negative, and (b) Influenza versus Other prediction
576 models on the internal validation test.



577

578 **Figure 3.** SHAP summary plot depicting the relative importance, impact and contribution of
579 different features on the output of (a) Influenza vs COVID-19-positive, (b) Influenza vs Other
580 and (c) COVID-19-positive vs COVID-19-negative predictive models.



581

582 **Figure 4.** SHAP explanations for observations from (a) Influenza A/B and (b) COVID-19-positive predictions. The underlying model
583 is XGBoost. Features that are contributing to a higher and lower probability are shown in red and blue, respectively along with the size
584 of each feature's contribution to the model output.

a. Influenza



b. COVID-19-positive



585

586

587 **Figure 5.** SHAP force plots of two patient encounters with (a) COVID-19-positive and (b) COVID-19-negative predictions. Features
 588 that are contributing to a higher and lower probability are shown in red and blue, respectively along with the size of each feature's
 589 contribution to the model output.

a. COVID-19-negative



b. COVID-19-positive



590

591 **Tables.**

TABLE 1. Demographics of WVU Patients (included COVID-19-positive, COVID-19-negative and Influenza cohort)

	Overall	COVID-19- positive	Influenza	COVID-19- negative	p value
N	3883	747	1223	1913	
Overall Age, in years	52 ± 24	55 ± 22 [*]	41 ± 24 [†]	57 ± 23	< 0.001 [‡]
Age by groups					< 0.001 [§]
Kids & Teens (0-20)	520	63 (8.4)	319 (26.1)	138 (7.2)	
Adults (21-44)	940	171 (22.9)	349 (28.5)	420 (22.0)	
Older Adults (45-64)	1005	216 (28.9)	282 (23.1)	507 (26.5)	
Seniors (65 or older)	1418	297 (39.8)	273 (22.3)	848 (44.3)	
Male, n(%)	1876	375 (50.2)	585 (47.8)	916 (47.9)	0.51
Race					< 0.001 [§]
			1037		
White/Caucasian, n(%)	3455	641 (85.8)	(84.8)	1777 (92.9)	
Black/African-American, n(%)	203	48 (6.43)	95 (7.8)	60 (3.1)	
Other, n(%)	225	58 (7.8)	91 (7.4)	76 (4.0)	
Ethnicity					< 0.001 [§]
Hispanic/Latino, n(%)	94	34 (4.6)	43 (3.5)	17 (0.9)	
			1180		
Other, n(%)	3789	713 (95.5)	(96.5)	1896 (99.1)	
Body Mass Index, kg/m²	30.0 ± 9.4	31.6 ± 8.8 ^{*†}	29.7 ± 9.5	29.6 ± 9.5	< 0.001 [‡]
Vitals, (mean±SD)					
Temperature in °F,	98.3 ± 1.1	98.3 ± 1.1 ^{*†}	99.0 ± 1.3 [†]	98.0 ± 0.8	< 0.001 [‡]
Systolic blood pressure, mmHg	126 ± 20	127 ± 19 [*]	124 ± 19 [†]	126 ± 20	0.004 [‡]
Diastolic blood pressure, mmHg	73 ± 13	75 ± 13 ^{*†}	72 ± 12	73 ± 13	< 0.001 [‡]
Heart rate, beats per minutes	87 ± 18	83 ± 16 [*]	94 ± 20 [†]	83 ± 17	< 0.001 [‡]
Oxygen Saturation (SpO ₂), %	96 ± 4	96 ± 4 ^{*†}	97 ± 3 [†]	96 ± 4	< 0.001 [‡]
Respiratory rate	19 ± 4	19 ± 4 [*]	19 ± 3 [†]	18 ± 5	< 0.001 [‡]

Values reported are counts (%) or mean ± standard deviation.

* p < 0.05 compared with the influenza group.

† p < 0.05 compared with the COVID-19-negative group.

‡ p < 0.05 using Kruskal Wallis test with Dunn-Bonferroni correction.

§ p < 0.05 using Chi-square test.

592

593

594 **TABLE 2.** Outcomes of WVU Patients presented at ED or admitted to WVU hospitals and
 595 tested positive for COVID-19, positive for Influenza A/B or negative for COVID-19.

	Overall	COVID-19-positive	Influenza	COVID-19-negative	p value
N	3883	747	1223	1913	
No. of ICU admissions, n (%)	655 (16.8)	142 (19.0)	70 (5.7)	443 (23.2)	< 0.001 [§]
Patient needing Ventilator, n (%)	264 (6.8)	43 (5.8)	39 (3.2)	182 (9.5)	< 0.001 [§]
No. of deaths, n(%)	261 (6.7)	51 (6.8)	51(4.2)	159 (8.3)	< 0.001 [§]
Age (in years) at death, mean±SD	72 ± 14	75 ± 14 [*]	69 ± 13	72 ± 14	0.02 [‡]

Values reported are counts (%) or mean ± standard deviation.

* p < 0.05 compared with the influenza group.

‡ p < 0.05 using Kruskal Wallis test with Dunn-Bonferroni correction.

§ p < 0.05 using Chi-square test.

596

597

598

599

600 **TABLE 3.** Performance metrics of different XGBoost models for predicting the given record as
601 COVID-19-positive or influenza when tested on Internal validation or test set.

Performance Measure	Influenza vs COVID-19-positive	Influenza vs Others	Covid-19-positive vs COVID-19-negative
AUC	0.988	0.987	0.972
Accuracy	0.949	0.937	0.922
F1 Score	0.929	0.909	0.861
Sensitivity (Recall)	0.938	0.931	0.849
Specificity	0.954	0.940	0.951
PPV (Precision)	0.920	0.887	0.873
NPV	0.965	0.964	0.941
FPR	0.046	0.060	0.049
FDR	0.081	0.113	0.127
FNR	0.062	0.069	0.151

602

603

604 **TABLE 4.** Performance of Influenza versus COVID-19-positive and Influenza versus Others
605 (COVID-19-positive/-negative) classification models on the external validation cohort.

Performance Measure	Influenza vs COVID-19-positive	Influenza vs Others
AUC	0.923	0.923
Accuracy	0.852	0.801
F1 Score	0.827	0.807
Sensitivity (Recall)	0.842	0.682
Specificity	0.860	0.989
PPV (Precision)	0.814	0.990
NPV	0.882	0.664
FPR	0.141	0.011
FDR	0.187	0.010
FNR	0.158	0.318

606